ARTICLE
Journal of Cellular Biochemistry 107:1189–1197 (2009)

Journal of Cellular Biochemistry

Effects of Fibre Type and Diffusion Distance on Mouse Skeletal Muscle Glycogen Content In Vitro

Peter Sogaard,[1,2] Ferenc Szekeres,[1] Maria Holmström,[1] Dennis Larsson,[2] Mikael Harlén,[3] Pablo Garcia-Roves,[1,4] and Alexander V. Chibalin[1*]

[1] *Department of Molecular Medicine and Surgery, Section of Integrative Physiology, Karolinska Institutet, Stockholm, Sweden*

[2] *Systems Biology Research Centre, Department of Biomedicine, University of Skövde, P.O. Box 408, 541 28 Skövde, Sweden*

[3] *Systems Biology Research Centre, Department of Cell and Molecular Biology, School of Life Sciences, University of Skövde, P.O. Box 408, 541 28 Skövde, Sweden*

[4] *Section of Integrative Physiology, Department of Physiology and Pharmacology, Karolinska Institutet, Stockholm, Sweden*

ABSTRACT

In vitro incubation of isolated rodent skeletal muscle is a widely used procedure in metabolic research. One concern with this method is the development of an anoxic state during the incubation period that can cause muscle glycogen depletion. Our aim was to investigate whether in vitro incubation conditions influence glycogen concentration in glycolytic *extensor digitorum longus* (EDL) and oxidative *soleus* mouse muscle. Quantitative immunohistochemistry was applied to assess glycogen content in incubated skeletal muscle. Glycogen concentration was depleted, independent of insulin-stimulation in the incubated skeletal muscle. The extent of glycogen depletion was correlated with the oxidative fibre distribution and with the induction of hypoxia-induced-factor-1-alpha. Insulin exposure partially prevented glycogen depletion in *soleus*, but not in EDL muscle, providing evidence that glucose diffusion is not a limiting step to maintain glycogen content. Our results provide evidence to suggest that the anoxic milieu and the intrinsic characteristics of the skeletal muscle fibre type play a major role in inducing glycogen depletion in during in vitro incubations. J. Cell. Biochem. 107: 1189–1197, 2009.

KEY WORDS: IMMUNOHISTOCHEMISTRY; MUSCLE GLYCOGEN; FIBRE TYPE; INSULIN ACTION; ANOXIA

Incubation of isolated skeletal muscle in an oxygenated solution is a commonly used method to study in vitro hormonal responses on metabolism. In vivo, the circulatory system provides sufficient oxygen and nutrient transfer deep within the tissues. During in vitro experiments, oxygen and nutrients are transferred to the skeletal muscle specimen by diffusion. To avoid local hypoxia deep within the muscle, perfusion systems [Bonen et al., 1994] or small skeletal muscle specimens [Henriksen and Holloszy, 1991] are generally used. During the in vitro incubation, the main assumption is that the diffusion distance to the internal core of the muscle specimen is short enough to secure a sufficient supply of oxygen and nutrients to prevent anoxia and energy depletion.

The two skeletal muscle types most commonly used that represent different fibre-type profiles in mouse models are the glycolytic *extensor digitorum longus* (EDL) and the oxidative *soleus* [Ariano et al., 1973]. These muscle specimens are composed of oxidative and glycolytic fibre types; approximately 80% of fibres in the EDL are glycolytic type IIB, whereas approximately 80% of the fibres in the *soleus* are oxidative type I [Girgenrath et al., 2005]. The fibre-type distribution is made up of an organised pattern of oxidative fibres that are assembled centrally within the muscle specimen [Hirofuji et al., 1992; Venema, 1995; Wang and Kernell, 2001a,b; Widmer et al., 2002].

Mathematical modelling of the oxygen diffusion capacity into the internal portion of the mouse EDL and *soleus* muscle during in vitro incubations provides evidence to suggest that the diffusion rate is sufficient for oxygenation of resting muscle [Barclay, 2005]. However, in vitro muscle contraction increases the rate of metabolism and oxygen consumption by the tissue, and consequently oxygen delivery deep within the muscle is insufficient [Barclay,

*Correspondence to: Dr. Alexander V. Chibalin, Section of Integrative Physiology, Department of Molecular Medicine and Surgery, von Eulers vag 4, 4 tr, Karolinska Institutet, 171 77 Stockholm, Sweden.
E-mail: alexander.chibalin@ki.se

Received 3 March 2009; Accepted 30 April 2009 • DOI 10.1002/jcb.22223 • © 2009 Wiley-Liss, Inc.
Published online 8 June 2009 in Wiley InterScience (www.interscience.wiley.com).

2005]. Immunohistochemical studies provide evidence for glycogen depletion within the muscle core after in vitro incubation [Maltin and Harris, 1985; van Breda et al., 1990], but this may be dependent upon intrinsic characteristics of the muscle specimens.

Here we test the hypothesis that the architecture or fibre-type composition of different muscle specimens may influence glycogen content during in vitro incubation conditions. To test this hypothesis, we applied a modified quantitative Periodic-Acid-Shiff (PAS) staining method [Schaart et al., 2004] to measure glycogen content in individual muscle fibres. We also determined the relationship between fibre-type composition and glycogen concentration in incubated muscle using predominantly glycolytic EDL and oxidative *soleus* muscle. Furthermore, we established whether fibre-type specific glycogen content is correlated with induction of hypoxia-induced-factor-1-alpha (HIF1-alpha) using a double staining protocol. Our results support earlier findings [Maltin and Harris, 1985; van Breda et al., 1990] of glycogen depletion in the inner-core of skeletal muscle after in vitro incubation. We observed glycogen depletion in the inner-core of EDL, but not *soleus* muscle after in vitro insulin-stimulation, compared to directly frozen muscle specimens. In EDL and *soleus* muscle, glycogen depletion was positively correlated with HIF1-alpha increased protein content after in vitro incubation. Interestingly, glycogen concentration was increased in the superficial fibres in *soleus*, but not in EDL muscle after the in vitro incubation in the absence of insulin. In conclusion, glycogen distribution in incubated skeletal muscle parallels the fibre-type dependent rate of glucose utilisation and the level of HIF1-alpha expression.

METHODS

CHEMICALS

All reagents were purchased from Sigma–Aldrich Chemical (St. Louis, MO), unless otherwise stated.

ANIMALS

The animal ethical committee of North Stockholm approved all experimental procedures. Mice were maintained in a temperature- and light-controlled environment with a 12:12 h light–dark cycle and had free access to standard rodent chow and water. C57Bl/6J mice were anaesthetized with Avertin (2,2,2-Tribromo ethanol, 99% and Tertiary amyl alcohol, 0.015–0.017 ml/g body weight) and EDL and *soleus* muscles were rapidly dissected. Muscles originating from the right or left leg were randomised for incubation in the presence or absence of insulin.

MUSCLE INCUBATIONS

Incubation media was composed of Krebs–Henseleit-bicarbonate (KHB) buffer containing 0.1% bovine serum albumin (RIA grade) [Wallberg-Henriksson et al., 1987]. Media were continuously gassed with 95% O_2/5% CO_2. Muscles were incubated for 10 min in a recovery solution containing KHB and 5 mM glucose and 15 mM mannitol. Thereafter, muscles were transferred to a fresh solution of KHB, 5 mM glucose and 15 mM mannitol and pre-incubated for 20 min in the absence or presence of insulin (12 nmol/L). Muscles were then rinsed in KHB containing 20 mM mannitol with no glucose for 10 min. Muscles were transferred to a final vial, containing KHB with 1 mM glucose and 19 mM mannitol and incubated for 20 min and thereafter, immediately frozen in isopentane chilled by liquid nitrogen. Muscles were stored at −80°C prior to analysis. Muscles were incubated for a total of 60 min and exposed to insulin during the final 50 min of the incubation protocol.

CRYOSTAT SECTIONING

Frozen muscle samples were mounted with a drop of OCT compound (Tissue-Tek, Sakura Finetek, NL) on pre-cooled and pre-holed cork plates. A thin layer of OCT was created to give the muscle support during the cryo-sectioning process. Sections of 14 μm were created on a Microm HM 500 M −23°C, mounted on SuperFrost (Menzel GmbH & Co.) microscopic slides and stored at −20°C until use.

PERIODIC-ACID-SHIFF (PAS) STAINING

Muscle glycogen was stained using a standard PAS protocol as follows: muscle sections were fixated for 1 h at 4°C in 3.7% (v/v) formaldehyde in 90% ethanol, pre-treated for 5 min with 1% (v/v) periodic acid, washed for 1 min with water, wash-dipped for 5 s in dH_2O, incubated in 1% Schiff's reagent for 15 min at room temperature, washed 5 s in dH_2O followed by 10 min in water with gentle agitation, and finally, washed five times in PBS. The slides were dehydrated 37°C for 30 min and the cover glass was mounted with Mountex (HistoLab Products, Sweden). To visualise the stained muscle sections, Axioscop2MOT (Carl Zeiss AB, Sweden), 2.5× was used with an Olympus DP70 camera (Olympus AB, Sweden) and CAST 2.3.1.6 software.

IMMUNOFLUORESCENCE AND DOUBLE STAINING

Immunofluorescence was used to detect the abundance of the HIF1-alpha (sc-10790) and caspase-3 (sc-7148) protein in the muscle sections. The Zenon Alexa Flour 555 rabbit IgG labelling reagent (Z-25305) was used (Invitrogen, Sweden). The following basic staining protocol with additions as previously described [Schaart et al., 2004] was used for the combination of immunofluorescence and PAS. Briefly a slide containing the frozen tissue section was thawed at room temperature for 15 min while borders were drawn with a PAP-pen (hydrophobic barrier pen for immunohistochemistry). Muscle sections were rehydrated with PBS for 15 min in room temperature. The sections were permeabilised at room temperature using PBS containing 0.2% Triton X-100 (PBT) for 20 min. Nonspecific binding sites were blocked with PBT containing 1% BSA for 30 min at room temperature, (Fig. 4D,H). Sections were incubated with antibody solution mixed in PBT for 2 h. The staining solutions were removed and sections washed in PBT three times for 15 min at room temperature. Sections were washed in PBS for two times at 5 min. A second fixation was performed by incubating samples with 4% formaldehyde in PBS for 15 min at room temperature. Sections were washed one more time with PBS for 5 min. Thereafter, the sections were mounted using ProLong Gold anti-fade reagent with DAPI (Invitrogen P36931, Sweden). The concentrations used for the antibody versus the Zenon Alexa Flour 555 rabbit IgG labelling reagent were 1:6 (antibody/labelling reagent) and diluted 1:6 (antibody mix/PBT) for the working

solution. Stained muscle sections were visualised using a confocal microscope (Inverted Zeiss LSM 510 META, Settings: Plane, multitrack, 12 bit, 1,024 × 1,024, 1,303.0 μm × 1,303.0 μm, Plan-Neufluar 100/0.3 and for the magnified images plane, multitrack, 12 bit, 1,024 × 1,024, 206.8 μm × 206.8 μm Plan-Apochromat 630/1.4 oil DIC.

GLYCOGEN MEASUREMENT

Muscle glycogen was analysed as previously described [Schaart et al., 2004]. A glycogen standard was used as a reference to estimate the glycogen concentration in the muscle sections. Several 4% gels (0.125 M Tris, 13.0% acrylamide (30:0.8%), 1.9% APS, 1.0% TEMED) were cast with a standard of known glycogen concentration. Gel specimens (~2 mm) in diameter, were isolated and frozen in OCT and sliced in 14 μm sections and subjected to PAS staining. A glycogen standard was prepared (Sigma G8751-5G; 0.200, 0.150, 0.100, 0.050, 0.025 and 0.000 M (blank)).

QUANTIFICATION OF PAS-STAINING

The settings for the microscope and camera were equal for all pictures taken. No background extraction was made. Each image was rotated, using Photoshop, so that the border facing the left side of the image was positioned without defects. A standardised region (50 × 200 pixels) was selected from three muscle sections from each animal, using MATLAB, (MathWorks, www.mathworks.com) (Fig. 1A).

STATISTICS

To estimate the mean intensity from the green channel in the image from PAS staining, three cryosections from the middle part of the whole muscle were selected. Three regions were analysed for each cryosection. The mean pixel intensity from all regions within one cryosection was calculated. An average of these three cryosections used to estimate muscle glycogen content from each muscle specimen. The data were handled in two different ways. (1) A vector with the mean-row-value was calculated from the matrix containing the mean values from the region, representing the glycogen measurement for each pixel. (2) The matrix was divided into eight groups; each group contained 25 mean-pixel-values, starting at the border of the standardised region with group X1. The mean value for each group represents an estimate for glycogen concentration in that position for each muscle specimen when the intensities were combined with the standard curve. To compare the within-muscle effect, normalisation against position X1 was performed and a Student's *t*-test was applied to test the hypothesis that no differences were expected. To compare between different treatments in the same group, X1–X8, normalisation was performed against muscle that was rapidly frozen without incubation (T0) at the corresponding group. A paired *t*-test was performed to test the following hypotheses: between T0 and muscle specimens incubated for 60 min without insulin (T60)—no differences was expected, for differences between T0, or T60 and incubation with insulin—an increase of glycogen was expected. An estimation of the glycogen concentration in the entire muscle was performed by taking the total mean value from the cryosections, tested for differences using a paired *t*-test.

RESULTS AND DISCUSSION

INCUBATION PROTOCOL

In this study we have utilized a standard protocol for in vitro glucose uptake in isolated mouse skeletal muscle [Barnes et al., 2004; Terada et al., 2006]. We have recapitulated all of the steps in the assay to further study the signalling mechanism behind the observed depletion of glycogen in the core of the muscle [Maltin and Harris, 1985; van Breda et al., 1990]. The first two in vitro incubation steps, recovery and pre-incubation, are believed to be important for recovery of the dissected muscle after the surgery. The next incubation step, incubation without glucose, is necessary to remove extracellular glucose from the muscle, because the glucose will compete with radiolabelled glucose analogue during the last incubation step. Mannitol is used to maintain the same osmolarity between all solutions. However, we cannot exclude the possibility that incubation without glucose can directly promote glycogen breakdown. At the last step of the procedure, the muscles were incubated in the presence of 1 mM glucose and 19 mM mannitol, according to the standard protocol.

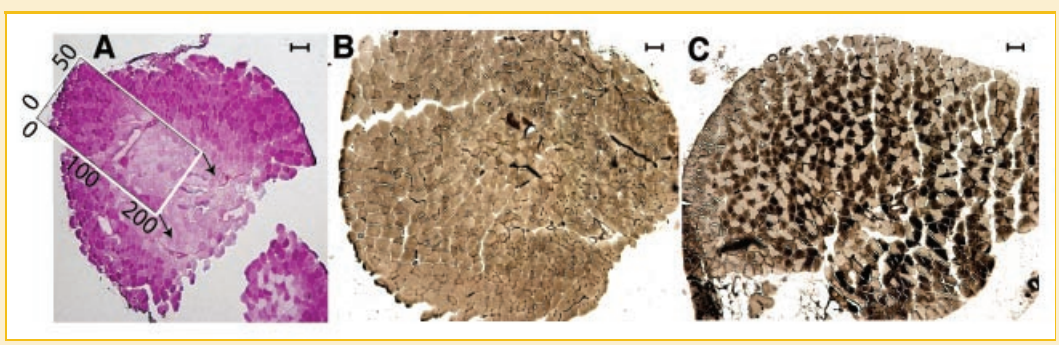

Fig. 1. Selection of a region within a muscle cross-section for statistical analysis and fibre-type characterisation. A: An example of the extracted region. Three regions of equal size were positioned to avoid artefact. B: Myosin ATPase staining of EDL muscle, at pH 4.55. C: Myosin ATPase staining of *soleus* muscle, at pH 10.60. Oxidative fibres stain darker than glycolytic fibres. The size bar is 100 μm.

DATA HANDLING FROM IMAGES

Glycogen concentration was determined as described [Schaart et al., 2004] with minor modifications, to evaluate the PAS stained images of the skeletal muscle sections. Earlier workers [Schaart et al., 2004] used the intensity of the greyscale channel combined with a standard curve as a measure of glycogen concentration. However, the greyscale is the weighted mean intensity value of red, green and blue channels from the RGB scale; thus, the greyscale is incompletely defined because different software programs use different weights to calculate the greyscale. To avoid this problem we used the green channel of the RGB scale, which is well defined for all software.

The selection of the region of the muscle that was subjected to statistical analysis is not straightforward. The cryosections were frequently frayed, and sometimes parts were missing (Figs. 1A and 2). Furthermore, the border of the sections was curved. To avoid unnecessary variance in the first columns of pixels due to background noise, all rows of pixels in the section of the images were aligned so that a specific threshold (210 on a 255 scale) of intensity was reached. The threshold was chosen as high as possible to distinguish between the background intensity and the portions of the muscle that was depleted of glycogen. However, there was still some variance in the first group, X1, due to threshold issues (Fig. 3A,E). The threshold selected ensured that the outer border was defined and that all rows in the corresponding matrix were starting at the edge of the muscle section. To determine the centre of the muscle cross-section, the width of several sections was determined. A selected distance of 200 pixels, corresponding to ~16 muscle fibres covering half the distance between the section borders was made (Fig. 1A).

The intensity of each pixel in the images was handled as a local measurement of glycogen concentration. This method allows for a statistical analysis of the data obtained from the images, and estimates the differences in glycogen concentration within or between the different muscle cryosections and the different treatment protocols.

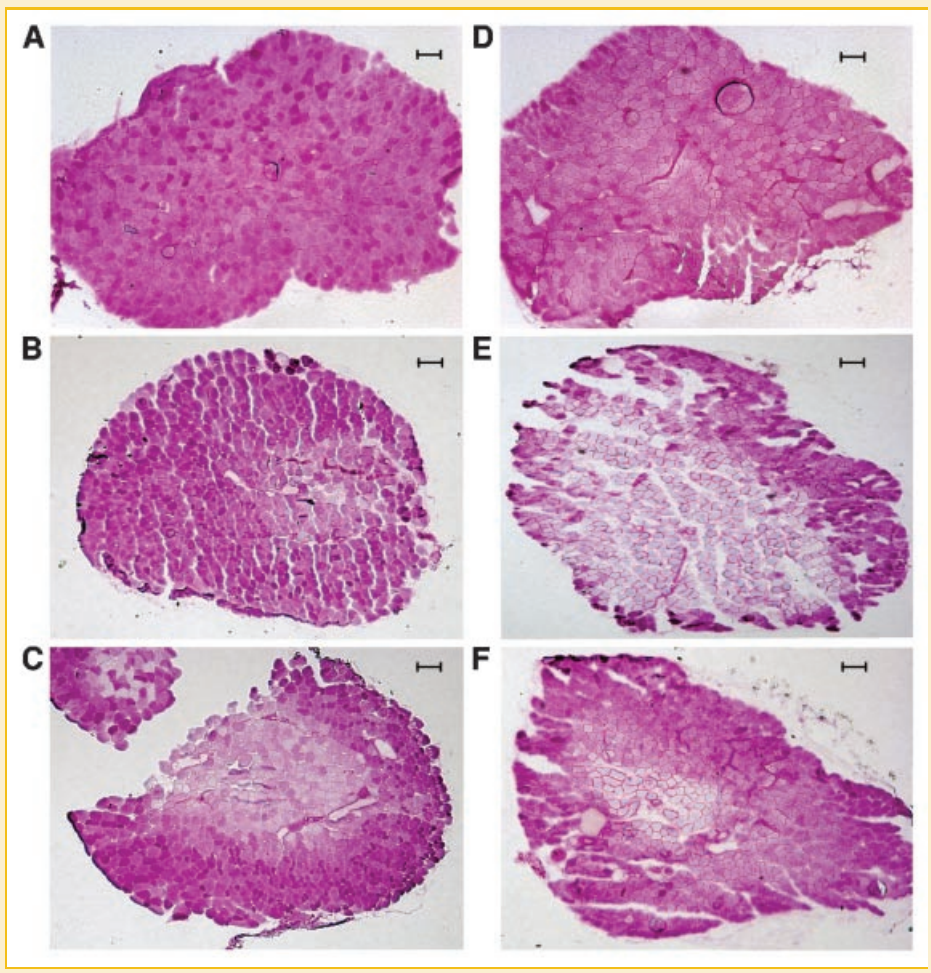

Fig. 2. Glycogen concentration in EDL and *soleus* muscle after incubation with or without insulin. Panels A–C show PAS-stained sections of EDL muscle. Panels D–F show PAS-stained sections of *soleus* muscle. Panels A and D show sections of control muscle (T0). Panels B and E show representative sections of muscle that were incubated for 60 min (T60). Panels C and F show sections of muscle that were incubated with insulin. The size bar is 100 μm. The images are from representative experiments repeated five to six times.

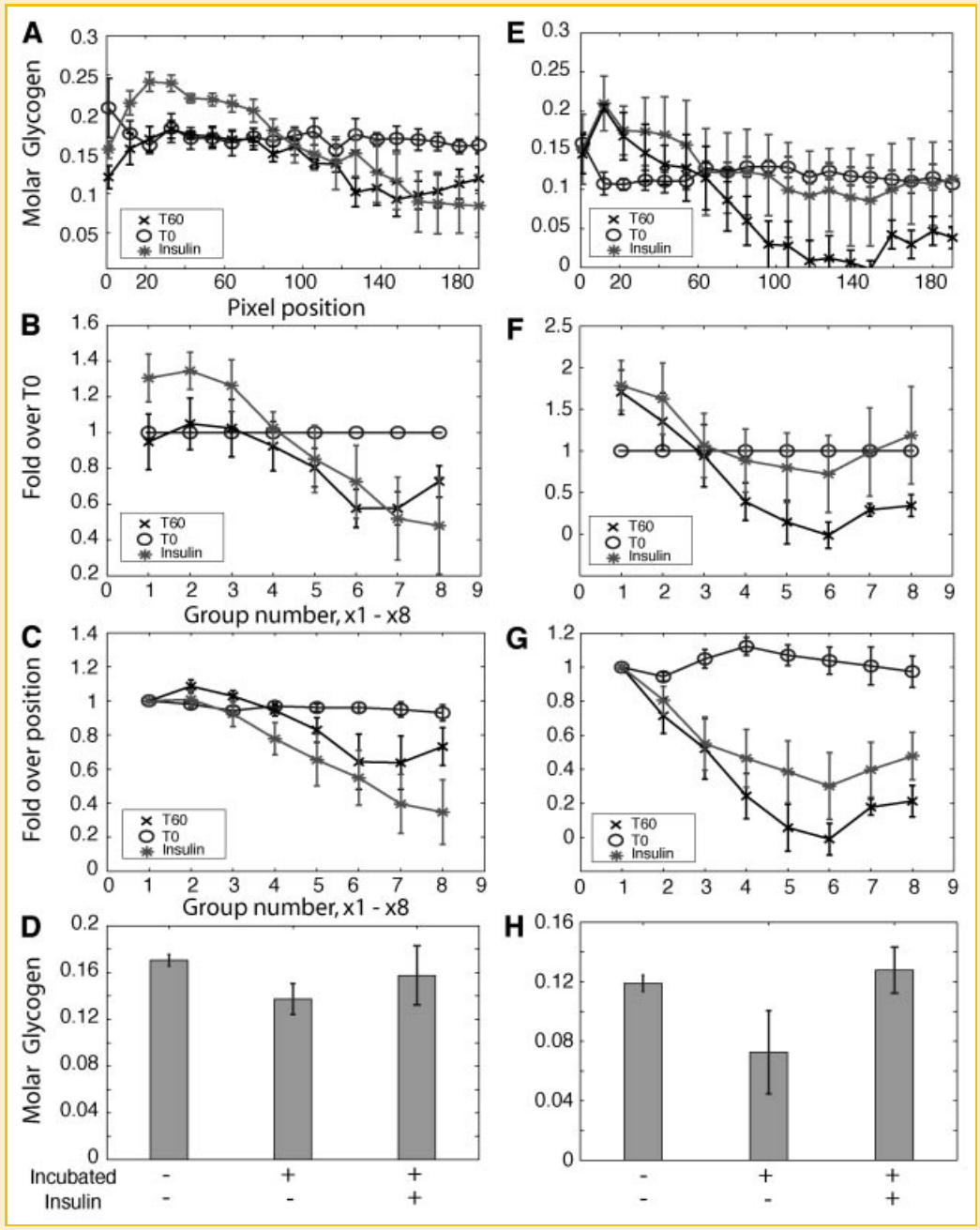

Fig. 3. Quantification of glycogen concentration from the muscle sections. Panels A–D show quantification of glycogen concentration in EDL muscle. Panels E–H show quantification of glycogen concentration in *soleus* muscle. Panels A and E show glycogen concentration measured in five muscles in each pixel position. Panels B and F show the grouped glycogen content normalised against each position in T0 (significance level is presented in Table II). Panels C and G show the grouped glycogen content normalised against position X1, (significance level is presented in Table I). Panels D and H show pooled concentration of glycogen from muscle sections (no significant differences were detected between any treatments). The diagram represents the mean ± SEM of five to six experiments.

GLYCOGEN DISTRIBUTION

PAS staining revealed differences in glycogen content due to fibre location, muscle treatment and muscle fibre type (Fig. 2). In muscles that were rapidly frozen after dissection (T0), normalisation against position X1 revealed no differences between adjacent fibres in either EDL or *soleus* muscle (Fig. 3C,G and Table I) indicating that glycogen concentration at the surface or the core of the muscle tissues was similar. These results support the applicability of this methodology for quantitative glycogen measurement [Schaart et al., 2004].

A trend for decreased glycogen concentration in the inner-core of the muscle was observed after normalisation against X1 for samples incubated in absence of insulin (T60). The decrease was significant

TABLE I. Fibre-Type Specific Changes in Glycogen Content

		Sample size, n	*P* values						
Muscle	Condition	n	X2	X3	X4	X5	X6	X7	X8
EDL	T0	5	0.27	0.09	0.17	0.14	0.26	0.31	0.21
	T60	4	0.11	0.45	0.18	0.10	0.11	0.10	0.10
	Insulin	4	0.87	0.39	0.10	0.11	0.07	**0.04**	**0.04**
Soleus	T0	5	0.09	0.42	0.08	0.31	0.65	0.95	0.79
	T60	4	0.07	0.07	**0.01**	**0.006**	**0.002**	**0.0004**	**0.003**
	Insulin	5	0.08	**0.04**	**0.03**	**0.03**	**0.02**	**0.02**	**0.02**

Results are shown as within differences. *P* values for the differences between position X1 and the mean in positions X2–X8. A two-tailed Student's *t*-test was performed. In the T0 condition, there was no deviation from position X1 detected in neither EDL nor *soleus*. However, in the other conditions a clear trend, EDL T60 or significant decrease of glycogen concentration was observed towards the interior of the muscle section.
Significant *P*-values are marked in bold.

for *soleus*, but not for EDL (Fig. 3C,G and Table I). Insulin exposure significantly decreased glycogen concentration in EDL and *soleus* muscle (Fig. 3C,G and Table I).

The mechanism for the observed glycogen depletion in the inner-core of the skeletal muscle during in vitro incubation is unclear. The decrease in muscle glycogen content could be due to impaired diffusion of oxygen, glucose or insulin, and/or the intrinsic consumption rate of the individual fibres. Diffusion rates for oxygen, glucose or insulin are unlikely to change during the incubation procedure. Rather, the glycogen depletion at the inner-core of the muscle specimen is likely to arise from metabolic changes at the level of the individual fibres. This change could be an arising of an anoxic milieu in the core of the muscle tissue.

The decrease in glycogen concentration in incubated muscle (T60) indicates that glucose uptake may be insufficient to compensate for glucose utilisation for energy production under the in vitro conditions. Thus, glycogenolysis may be increased under these conditions. This hypothesis is consistent with predictions from mathematical analyses (P. Sogaard, unpublished observation). Furthermore, increased glycogenolysis would most likely lead to a decrease in muscle glycogen concentration (Fig. 3).

Our findings are consistent with earlier reports indicating oxidative fibres are more insulin sensitive than glycolytic fibres [Song et al., 1999], which suggests glycogen content is rapidly increased in oxidative fibres due to increased glucose uptake. The centrally located type I fibres in *soleus* muscle are more oxidative than the centrally located type IIA fibres in EDL muscle [Schiaffino and Reggiani, 1994]. A trend for increased glycogen content in *soleus*, but not EDL muscle was observed (Fig. 3B,F and Table II), despite similar diffusion distances. The ability of insulin to diffuse into the internal fibres and trigger signal transduction was unaffected (P. Sogaard, unpublished observation). Thus, we speculate that the increase in glycogen concentration following insulin-stimulation in *soleus* muscle compared to T60 provides evidence that glucose diffusion is not a limiting factor for glucose utilisation (Fig. 3 and Table II). However, comparison of glycogen content within the same treatment and muscle type reveals a spatial decrease of glycogen concentration for both EDL and *soleus* muscles (Fig. 3C,G and Table I), indicating that additional signalling pathways are involved in the regulation of the glycogen content. We found that HIF1-alpha- and caspase-3-dependent signalling is activated in inner-core of the muscle (Figs. 4 and 6). These pathways are associated with an increase in glycogen breakdown [Hilder et al., 2005; Krohn et al., 2008].

An alternative explanation for the difference in glycogen concentration between T60 and the insulin-stimulated conditions could be related to increased lipid oxidation in *soleus* muscle, which would decrease the demand for energy production from glucose. Thus, the glucose flux would then be directed towards glycogen synthesis. However, our results strongly challenge this hypothesis, since HIF1-alpha content was increased after incubation with or without insulin in EDL (Fig. 4A–C) and *soleus* (Fig. 4E–G) muscle, providing evidence that lipid oxidation is limited.

An anoxic milieu increases glycolysis [Krohn et al., 2008] when energy demand is increased. The increased energy demand increases pyruvate fermentation, thereby producing ATP and lactate. Lactate concentration is increased after incubation in the absence [Bonen et al., 1994; Tsao et al., 2001] or presence

TABLE II. Glycogen Content in Incubated EDL or *Soleus* Skeletal Muscle in the Absence or Presence of Insulin

			P values							
Muscle	Conditions	Hypothesis (H0)	X1	X2	X3	X4	X5	X6	X7	X8
EDL	T0 vs. T60	No differences	0.76	0.75	0.89	0.62	0.17	**0.03**	**0.02**	0.05
	T0 vs. insulin	Increase	0.05	**0.02**	0.08	0.40	0.75	0.87	0.93	0.92
	T60 vs. insulin	Increase	0.07	0.07	0.15	0.28	0.42	0.27	0.58	0.78
Soleus	T0 vs. T60	No differences	0.08	0.38	0.88	0.07	**0.04**	**0.007**	**0.002**	**0.01**
	T0 vs. insulin	Increase	**0.03**	0.11	0.44	0.61	0.67	0.71	0.51	0.38
	T60 vs. insulin	Increase	0.42	0.32	0.41	0.15	0.11	0.09	0.13	0.11

Results are reported as between differences. *P* values for difference between treatments. The tested hypothesis was different depending on the response that was expected from the treatment. When no difference is stated, a two-tailed test was performed, and, when increase is stated, a right side *t*-test was performed.
Significant *P*-values are marked in bold.

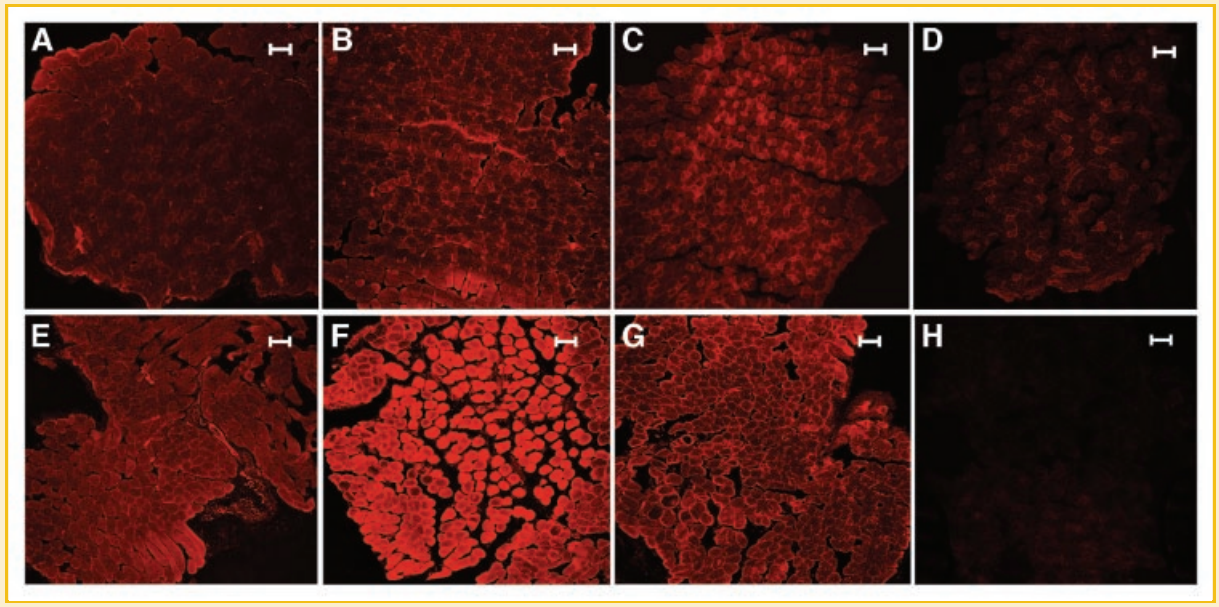

Fig. 4. Immuno staining of HIF1 alpha induction in EDL and *soleus* muscles within muscle sections. Muscle sections were frozen and sectioned before or after the 60 min incubation in the absence (panels B and E) or in presence (panels C and F) of insulin, as described in the Methods Section. Staining for HIF1-alpha was performed on EDL (panels A–C) and *soleus* (panels D–F) muscle. As a negative control, HIF1-alpha staining was performed as a negative control on muscle sections that were frozen immediately after surgery, and results are shown in panels A and D. The images shown are from representative experiments repeated five to six times. The size bar is 100 μm. In panel D auto-fluorescence is observed, which is blocked with BSA (panel H), as described in 'Methods Section'.

(P. Sogaard, unpublished observation) of insulin. However, the fermentation of pyruvate is an inefficient way of producing ATP and increases the demand of available substrates; consequently glycogenolysis may be increased.

To further investigate whether glucose uptake is insufficient to supply the increased flux through glycolysis and the fermentation of pyruvate to lactate, causing glycogen depletion, we applied a double staining procedure against glycogen and HIF1-alpha in the muscle

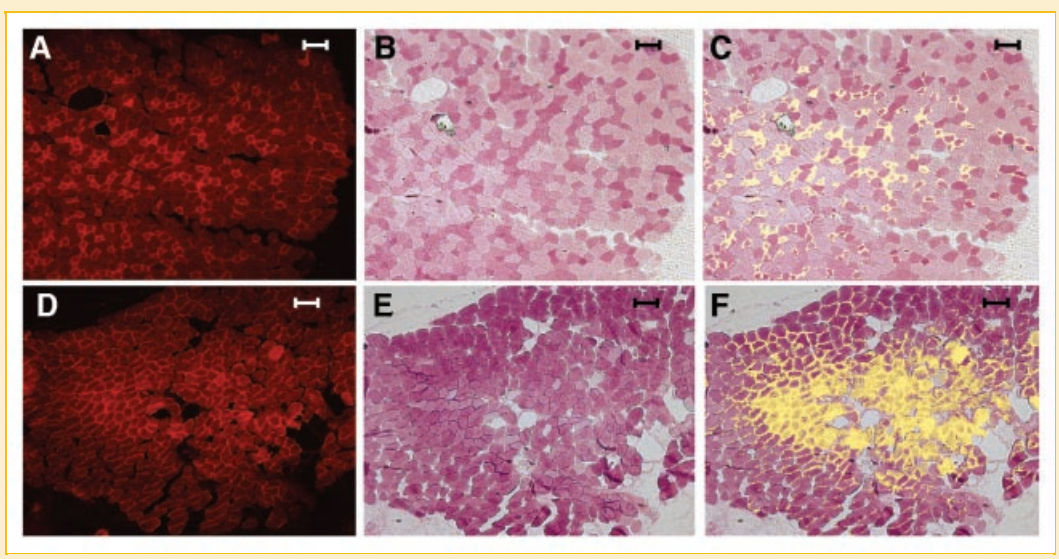

Fig. 5. HIF1-alpha induction correlates with the glycogen-depleted regions within the muscle sections. Muscle sections were frozen and sectioned after the 60 min incubation with or without insulin, as described in the Methods Section. A double staining against glycogen and HIF1-alpha was performed. Panels A–C show data for EDL muscle and D–F show data for *soleus* muscle. Panels B and E show staining for glycogen, A and D is HIF1-alpha staining (red) and, C and F is the merged pictures. In the merged images, the colour was changed for HIF1-alpha from red to yellow for clarity; furthermore, only red intensity beyond 80 has been extracted from the panels A and D, respectively. The images shown are from representative experiments repeated five to six times. The size bar is 100 μm.

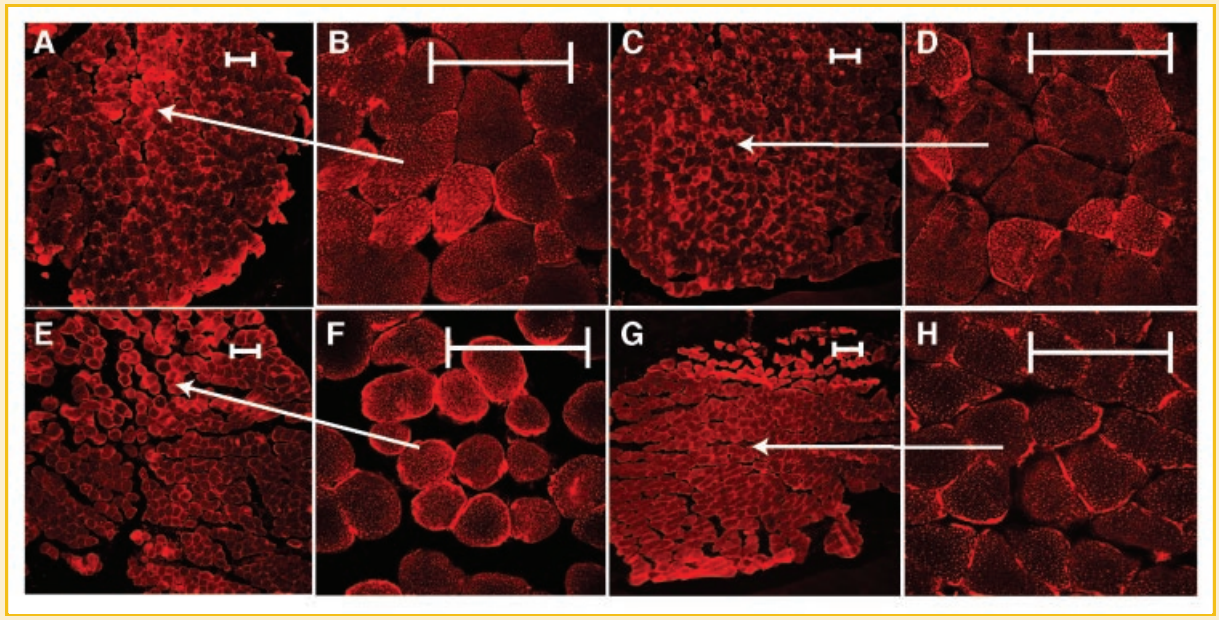

Fig. 6. Caspase-3 induction is increased centrally in incubated muscles. Muscle sections were frozen and sectioned after the 60 min incubation with or without insulin, as described in the Methods Section. Staining for caspase-3 was performed on EDL (panels A and D) and *soleus* (panels E and H) muscles. The 630 magnification (panels B, D and F, H) is from the centre of the section as shown in panel A, D and E, G, respectively. Panels A, B and E, F are images from muscles incubated without insulin, whereas panels C, D and G, H are images from muscles incubated with insulin. The images shown are from representative experiments repeated five to six times. The size bar is 100 μm.

cryosections (Schaart et al., 2004). A clear spatial dependent pattern for glycogen content and HIF1-alpha expression was observed in both muscle types (Figs. 4 and 5). At the level of single fibres, a correlation was observed between the degree of HIF1-alpha induction and glycogen content in EDL (Fig. 5A–C) and *soleus* (Fig. 5D–F) muscle.

Moreover, sever energy depletion can directly induce apoptosis [Hilder et al., 2005]. The cleaved form of caspase-3 was used as a marker for induced apoptotic signalling pathway [Cohen, 1997]. Protein content of caspase-3 was increased centrally in the muscles studied (Fig. 6), similarly to the pattern observed for both glycogen and HIF1-alpha. In *soleus* muscle (Fig. 6E–H), a decrease of caspase-3 staining was observed after insulin-stimulation, concomitant with a protective effect of insulin against glycogen depletion (Fig. 3G). The apoptotic process requires energy and an increase in the activity of apoptotic pathways can increase glycogen degradation to maintain ATP levels [Hilder et al., 2005]. Indeed, the ATP concentration has been reported to be unchanged during similar in vitro skeletal muscle incubations [Newsholme et al., 1986].

The increase in glycogen in the superficial fibres of the *soleus* muscle at T60 (Fig. 3E,F and Table II) was unexpected, and the molecular mechanism for this change is incompletely understood. Possible explanations may be either a response to stress from the handling the muscles during surgery or the effect of the low glucose concentration to auto-regulate glucose uptake [Itani et al., 2003]. Furthermore, the recovery step may be insufficient because glycogen content was increased at the superficial fibres in nonstimulated *soleus* muscle (Fig. 3E,F). However, in EDL muscle, the pattern of glycogen staining after the 60 min incubation indicates that glucose and oxygen was sufficient to maintain the glycogen concentration in the superficial fibres (Fig. 3A,B and Table II). Furthermore, decline in glycogen concentration was observed beyond the superficial cells in the deeper layer of fibres in *soleus*, but not EDL muscle, indicating that induction of hypoxia was more pronounced in type IIA fibres of *soleus*, rather than type IIB of EDL (Figs. 1B,C, 3A–C,E–G and 5C).

When whole muscle preparations are homogenised and used for subsequently measurements, the assumption is made that most of the individual muscle fibres act in a homologous manner upon stimulation. However, in a heterogeneous sample, such as in EDL and *soleus* muscle, a method with higher resolution might be more appropriate to study metabolic events. The increased resolution that can be achieved through quantitative immunohistochemistry of muscle sections indicates that changes in glycogen concentration can be observed between the spatial and mean value, despite similar amount of total glycogen concentration (Fig. 3D,H). The finding of unaltered glycogen concentration is consistent with previous observations [Tsao et al., 2001].

CONCLUSION

We used immunohistochemistry to quantify glycogen concentration within skeletal muscle composed of different fibre types. The intensity within the images was quantified with a novel method that allows for the study of the spatial effects of the incubation condition(s) on glycogen content. Furthermore, we studied the induction of HIF1-alpha and caspase-3 on a single-cell-level within the tissue. In conclusion, in vitro incubation of isolated skeletal muscles is associated with glycogen depletion in the inner-core of

the muscle. The cross-sectional area of the glycogen-depleted muscle fibres correlates with the distribution of oxidative fibres in the inner-core of the muscle specimen, as well as increased HIF1-alpha protein content. The conventional averaging that is performed when homogenizing the tissue before biochemical measurement masks the essential molecular mechanism behind the glycogen-depleted core formation. Supplementary higher-resolution methods may offer a complementary method to assess fibre-type specific effects on glucose homeostasis in incubated muscle.

ACKNOWLEDGMENTS

The authors thank Professor Juleen R. Zierath helpful discussions throughout the study. This study was supported by grants from the Swedish Knowledge Foundation through the Industrial PhD programme in Medical Bioinformatics at Karolinska Institutet, Strategy and Development Office, the Swedish Research Council, Swedish Medical Association, the Novo-Nordisk Foundation, and the Swedish Diabetes Association. Swedish Diabetes Association, and the commission of the European Communities (Contract No. LSHM-CT-2004-512013 EUGENEHEART and Contract No. LSHM-CT-2004-005272 EXGENESIS).

REFERENCES

Ariano MA, Armstrong RB, Edgerton VR. 1973. Hindlimb muscle fiber populations of five mammals. J Histochem Cytochem 21:51–55.

Barclay CJ. 2005. Modelling diffusive O(2) supply to isolated preparations of mammalian skeletal and cardiac muscle. J Muscle Res Cell Motil 26:225–235.

Barnes BR, Marklund S, Steiler TL, Walter M, Hjalm G, Amarger V, Mahlapuu M, Leng Y, Johansson C, Galuska D, Lindgren K, Abrink M, Stapleton D, Zierath JR, Andersson L. 2004. The 5'-AMP-activated protein kinase gamma3 isoform has a key role in carbohydrate and lipid metabolism in glycolytic skeletal muscle. J Biol Chem 279:38441–38447.

Bonen A, Clark MG, Henriksen EJ. 1994. Experimental approaches in muscle metabolism: Hindlimb perfusion and isolated muscle incubations. Am J Physiol 266:E1–E16.

Cohen GM. 1997. Caspases: The executioners of apoptosis. Biochem J 326(Pt 1): 1–16.

Girgenrath S, Song K, Whittemore LA. 2005. Loss of myostatin expression alters fiber-type distribution and expression of myosin heavy chain isoforms in slow- and fast-type skeletal muscle. Muscle Nerve 31:34–40.

Henriksen EJ, Holloszy JO. 1991. Effect of diffusion distance on measurement of rat skeletal muscle glucose transport in vitro. Acta Physiol Scand 143:381–386.

Hilder TL, Carlson GM, Haystead TA, Krebs EG, Graves LM. 2005. Caspase-3 dependent cleavage and activation of skeletal muscle phosphorylase b kinase. Mol Cell Biochem 275:233–242.

Hirofuji C, Ishihara A, Itoh K, Itoh M, Taguchi S, Takeuchi-Hayashi H. 1992. Fibre type composition of the *soleus* muscle in hypoxia-acclimatised rats. J Anat 181(Pt 2): 327–333.

Itani SI, Saha AK, Kurowski TG, Coffin HR, Tornheim K, Ruderman NB. 2003. Glucose autoregulates its uptake in skeletal muscle: Involvement of AMP-activated protein kinase. Diabetes 52:1635–1640.

Krohn KA, Link JM, Mason RP. 2008. Molecular imaging of hypoxia. J Nucl Med 49(Suppl 2): 129S–148S.

Maltin CA, Harris CI. 1985. Morphological observations and rates of protein synthesis in rat muscles incubated in vitro. Biochem J 232:927–930.

Newsholme EA, Leighton B, Challiss RA, Lozeman FJ. 1986. Assessment of biochemical viability of isolated incubated muscle preparations. Biochem J 238:621–622.

Schaart G, Hesselink RP, Keizer HA, van Kranenburg G, Drost MR, Hesselink MK. 2004. A modified PAS stain combined with immunofluorescence for quantitative analyses of glycogen in muscle sections. Histochem Cell Biol 122:161–169.

Schiaffino S, Reggiani C. 1994. Myosin isoforms in mammalian skeletal muscle. J Appl Physiol 77:493–501.

Song XM, Ryder JW, Kawano Y, Chibalin AV, Krook A, Zierath JR. 1999. Muscle fiber type specificity in insulin signal transduction. Am J Physiol 277:R1690–R1696.

Terada S, Wicke S, Holloszy JO, Han DH. 2006. PPARdelta activator GW-501516 has no acute effect on glucose transport in skeletal muscle. Am J Physiol Endocrinol Metab 290:E607–E611.

Tsao TS, Li J, Chang KS, Stenbit AE, Galuska D, Anderson JE, Zierath JR, McCarter RJ, Charron MJ. 2001. Metabolic adaptations in skeletal muscle overexpressing GLU T4: Effects on muscle and physical activity. FASEB J 15:958–969.

van Breda E, Keizer HA, Glatz JF, Geurten P. 1990. Use of the intact mouse skeletal-muscle preparation for metabolic studies. Evaluation of the model. Biochem J 267:257–260.

Venema HW. 1995. Spatial distribution of muscle fibers. Anat Rec 241:288–290.

Wallberg-Henriksson H, Zetan N, Henriksson J. 1987. Reversibility of decreased insulin-stimulated glucose transport capacity in diabetic muscle with in vitro incubation. Insulin is not required. J Biol Chem 262:7665–7671.

Wang LC, Kernell D. 2001a. Fibre type regionalisation in lower hindlimb muscles of rabbit, rat and mouse: A comparative study. J Anat 199:631–643.

Wang LC, Kernell D. 2001b. Quantification of fibre type regionalisation: An analysis of lower hindlimb muscles in the rat. J Anat 198:295–308.

Widmer CG, Morris-Wiman JA, Nekula C. 2002. Spatial distribution of myosin heavy-chain isoforms in mouse masseter. J Dent Res 81:33–38.